Field dependence of the paramagnetic susceptibility of the antiferromagnets $CoCl_2 \cdot 6H_2O$, $NiCl_2 \cdot 4H_2O$, $MnCl_2 \cdot 4H_2O$, and $MnBr_2 \cdot 4H_2O$

S. S. Vianna
Departamento de Física, Universidade Federal de Pernambuco, 50000 Recife, Pernambuco, Brazil

C. C. Becerra
Instituto de Física, Universidade de São Paulo, 20516 São Paulo, São Paulo, Brazil

(Received 20 September 1982)

We report differential paramagnetic susceptibility (χ) measurements as a function of an applied magnetic field (H) for the antiferromagnets $CoCl_2 \cdot 6H_2O$, $NiCl_2 \cdot 4H_2O$, $MnCl_2 \cdot 4H_2O$, and $MnBr_2 \cdot 4H_2O$. Above the ordering temperature, the χ vs H curves exhibit a characteristic maximum which is attributed to short-range order. This effect is more pronounced in the cobalt compound (spin $\frac{1}{2}$) and less pronounced in the manganese compounds (spin $\frac{5}{2}$). Using simple models suitable to describe the above-mentioned systems, we discuss the dependence of this maximum with spin magnitude, anisotropy, and lattice dimensionality. The theoretical treatment is based on a variational method in which correlation effects between pairs of spins are considered.

I. INTRODUCTION

The theoretical treatments based on mean-field approximations (MFA) predict that above the ordering temperature T_N of an antiferromagnet, the magnetic susceptibility χ as a function of a magnetic field $\vec{H}$ applied along the easy-magnetization axis should decrease with increasing H. However, the experimental data for a variety of antiferromagnets[1-3] show that, in the paramagnetic phase, the behavior of the susceptibility is not in accordance with this MFA prediction. In fact, it is observed that at (fixed) temperatures just above T_N, the χ vs H curves exhibit a broad maximum which gradually decreases in field value and turns less pronounced with increasing temperature. The occurrence of this maximum can be explained[4] by considering correlation effects which are neglected in MFA.

In this paper we shall investigate the behavior of the susceptibility in the paramagnetic phase of the antiferromagnets $CoCl_2 \cdot 6H_2O$, $NiCl_2 \cdot 4H_2O$, $MnCl_2 \cdot 4H_2O$, and $MnBr_2 \cdot 4H_2O$. These materials have different spin magnitudes, and the mechanisms that account for their magnetic anisotropy are distinct. Also, $CoCl_2 \cdot 6H_2O$ behaves as a two-dimensional system, whereas the other three compounds exhibit three-dimensional behavior. Previous measurements[1-3,5-8] of the field dependence of χ have been mainly used to derive the phase diagrams of the compounds. In an attempt to understand the dependence of the susceptibility on the spin magnitude, anisotropy, and dimensionality, we compare the susceptibility data with theoretical predictions derived from simple models suitable to describe the above-mentioned systems. This has been done by applying a procedure developed by Ferreira *et al.*,[4] which is based on a variational principle for the free energy. It involves the choice of a suitable parametrized trial Hamiltonian which systematically takes into account correlation effects in increasing degree of complexity. In this paper we consider correlation effects at the lowest order, i.e., between pairs of spins. As shown by Ferreira *et al.*,[4] in the case of the three-dimensional antiferromagnet Heisenberg model this led to a maximum in the χ vs H curves. These comparisons, however, are only qualitative in character and should be viewed as indicative.

The remainder of this paper is divided as follows: In Sec. II we discuss the theoretical background and present an outline of the variational method used to treat the correlation effects. In Sec. III we give details of the magnetic properties of the systems and of the experimental setup. The experimental results are presented in Sec. IV. Finally, a discussion of these results in connection with the theoretical predictions is made in Sec. V.

II. THEORY

A. Hamiltonians

We consider spin-localized Hamiltonians in which the spin system in the ordered phase is composed of two equivalent sublattices coupled antiferromagnetically. Experimental evidence[5] indicates that $CoCl_2 \cdot 6H_2O$ is a fairly good example of a two-dimensional antiferromagnet with spin $S=\frac{1}{2}$, in which the dominant interactions are of the planar type (two-dimensional XY model). Accordingly, we will consider the Hamiltonian

$$H_1 = -J_1 \sum_{(i,j)} (S_i^x S_j^x + S_i^y S_j^y) - \gamma_1 \sum_i S_i^x , \tag{1}$$

where the first term represents the quasi-isotropic superexchange coupling between the magnetic ions [(i,j) indicates a sum over nearest-neighbor pairs] and the second term is the Zeeman energy ($\gamma_1 = g_1 \mu_B H$).

The main source of the anisotropy in $NiCl_2 \cdot 4H_2O$ is of the single-ion type.[6] In this material the effect of the axial crystal field on the Ni^{2+} ion is to split the threefold-degenerate ground state into a doublet and a singlet, separated by an energy D. The spin Hamiltonian appropriate to describe this spin-1 system is

$$H_2 = -J_2 \sum_{\alpha=x,y,z} \sum_{(i,j)} S_i^\alpha S_j^\alpha - \sum_i [D (S_i^z)^2 + \gamma_2 S_i^z] . \tag{2}$$

In the manganese compounds $MnCl_2 \cdot 4H_2O$ and $MnBr_2 \cdot 4H_2O$ the anisotropy is due to anisotropic exchange and dipolar magnetic interactions[7,8] (S state with spin $\frac{5}{2}$). However, to study the effect of its high spin value, and to simplify the theoretical analysis, we shall consider a classical Heisenberg model (spin $\rightarrow \infty$) in the form

$$H_3 = -J_3 \sum_{\alpha=x,y,z} \sum_{(i,j)} s_i^\alpha s_j^\alpha - \gamma_3 \sum_i s_i^z , \tag{3}$$

where s_i^α are continuous variables in the interval $[-1,1]$.[9]

B. Variational method

We applied the variational method developed by Ferreira *et al.*[4] to the above-mentioned Hamiltonians. The procedure permits the inclusion of short-range-order effects through the choice of a suitable parametrized trial Hamiltonian which contains some elementary interactions. The free trial Hamiltonian leads to the usual MFA. When the trial Hamiltonian includes a certain number of pair interactions, the results obtained in the constant-coupling approximation[10] are recovered. This can be done by choosing the number of interacting pairs through a comparison with the first few terms of the exact high-temperature expansion of the free energy.

Let us illustrate the main steps of the procedure for an antiferromagnetic spin-$\frac{1}{2}$ Heisenberg model with isotropic exchange interactions ($J<0$). We divide the lattice into two sublattices, A and B, and construct a trial density matrix ρ_0 containing n linked pairs and $N-2n$ free spins. The trial Hamiltonian $\mathscr{H}_0$ is thus written

$$\mathscr{H}_0 = \mathscr{H}_{0f} + \mathscr{H}_{0p} , \tag{4}$$

where $\mathscr{H}_{0f}$ involves the $(N-2n)$ free spins and $\mathscr{H}_{0p}$ the n linked pairs. They are given, respectively, by

$$\mathscr{H}_{0f} = -\sum_A H_1^A S_z^A - \sum_B H_1^B S_z^B , \tag{5}$$

$$\mathscr{H}_{0p} = \sum_{\text{pairs}} (-H_2^A S_z^A - H_2^B S_z^B - J \vec{S}_A \cdot \vec{S}_B) , \tag{6}$$

where S_z^A and S_z^B are the spin components along the direction of the applied magnetic field. The sums extend over the A and B sublattices, and the pair interactions are between spins on different sublattices only. The four parameters H_1^A, H_1^B, H_2^A, and H_2^B (molecular fields) are determined from the conditions

$$\langle S_z^A \rangle \equiv \mathrm{Tr} \rho_0 S_z^A , \tag{7a}$$

$$\langle S_z^B \rangle \equiv \mathrm{Tr} \rho_0 S_z^B , \tag{7b}$$

regardless of whether the spin is isolated or belongs to a pair, and the minimization of the free energy $\phi = F_0 + \langle \mathscr{H} - \mathscr{H}_0 \rangle_0$, where F_0 is the free energy associated with the trial Hamiltonian $\mathscr{H}_0$. These conditions yield four equations. The number n of pairs is chosen so that a good approximation for the free energy is obtained. This is done by comparing the first terms of the high-temperature series expansion, for the true free energy F, with the free energy ϕ. In the high-temperature limit this procedure gives $n = Nq/2$, where q is the number of nearest neighbors. This choice of n leads, for $H=0$, to the relation

$$H_1^A / q = H_2^A / (1-q) , \tag{8}$$

and to an identical relation for the B sublattice. This leads to a set of thermodynamical functions which are identical to those obtained in the constant-coupling approximation and the Bethe-Peierls method.[10] In particular, the field dependence of the paramagnetic susceptibility, at constant temperature $T \gtrsim T_N$, displays a broad maximum, instead of decreasing monotonically with H as predicted by the standard MFA. We extended the above

procedure to the following models: (a) planar XY ($q=4$) model with $S=\frac{1}{2}$; (b) tridimensional Heisenberg model ($q=6$) with $S=1$; (c) tridimensional Heisenberg model with classical spins ($S=\infty$). We also included the effect of a single-ion anisotropy term in the $S=1$ Heisenberg model. Some details of the calculations are presented in Appendixes A, B, and C, and the results are discussed, in connection with the experimental data, in Sec. V.

III. EXPERIMENTAL

A. Samples

Single crystals of the four compounds were grown from saturated aqueous solutions. $MnCl_2\cdot 4H_2O$, $MnBr_2\cdot 4H_2O$, and $CoCl_2\cdot 6H_2O$ were grown at room temperature and $NiCl_2\cdot 4H_2O$ was grown in a temperature-controlled bath at a temperature of 50.0 ± 0.05 °C. The identification of the crystallographic axes was done from the crystal habit described by Groth.[11]

The antiferromagnet $CoCl_2\cdot 6H_2O$ (effective spin $S=\frac{1}{2}$) has a Néel temperature T_N of 2.29 K.[12] The structure of this compound is base-centered monoclinic, with two formula units per unit cell. The magnetic measurements[13] indicate that bc is an easy plane of magnetization and that b is the easy-magnetization axis. The two-dimensional character of the magnetic behavior of $CoCl_2\cdot 6H_2O$ has previously been inferred from the relatively large amount of short-range order that is present above T_N, as is evidenced by the specific-heat measurements[5,12] and from the temperature dependence of the antiferromagnetic susceptibility whose maximum occurs at about 40% above T_N.[6]

The antiferromagnets $MnCl_2\cdot 4H_2O$ and $MnBr_2\cdot 4H_2O$ ($S=\frac{5}{2}$) are isomorphous,[14] with T_N at 1.62 and 2.13 K, respectively. These crystals have monoclinic structure with four Mn^{2+} ions per unit cell.[11] Their magnetic structure is reported to be identical to the crystallographic one, with c being approximately the easy-magnetization axis.[15] Their anisotropy is mainly due to exchange and dipolar interactions.

The antiferromagnet $NiCl_2\cdot 4H_2O$ ($T_N=2.99$ K) is reported to be structurally and magnetically isomorphous to $MnCl_2\cdot 4H_2O$. It is described as a $S=1$ system in which the anisotropy is of the single-ion type with $D/|J|\cong 1.2$ K.[16]

B. Susceptibility measurements

The magnetic differential susceptibility (χ) was measured with an ac mutual inductance bridge similar to that described by Maxwell.[17] The frequency of the modulation field was 1550 Hz and its amplitude was 3 Oe. Checks made with frequencies of 155 Hz showed that the features of the χ vs H curves are independent of the measuring frequency. The magnetic field was provided by a high-homogeneity NbTi superconducting magnet.

The data for χ were taken in the helium temperature range with a cryogenic arrangement identical to that described by Oliveira, Jr. and Quadros.[18] The sample was immersed in the ^{4}He bath. During the run the temperature was kept fixed and the magnetic field was swept. The temperature was measured with a 10-Ω, 0.125-W Allen-Bradley carbon-resistance thermometer at the beginning and at the end of each run. While the field was swept the stability of the temperature was monitored with the vapor pressure of the ^{4}He with a differential manometer. The error of the temperature measurements did not exceed 0.01 K.

IV. EXPERIMENTAL RESULTS

Figures 1–4 show typical χ vs H curves for the four compounds. The magnetic field was always applied along the easy-magnetization axis. During each run the temperature was fixed. The temperature in which each curve was obtained is given through the ratio T/T_N. The common feature of these curves is the broad maximum observed in the paramagnetic phase for $T\gtrsim T_N$. These maxima in-

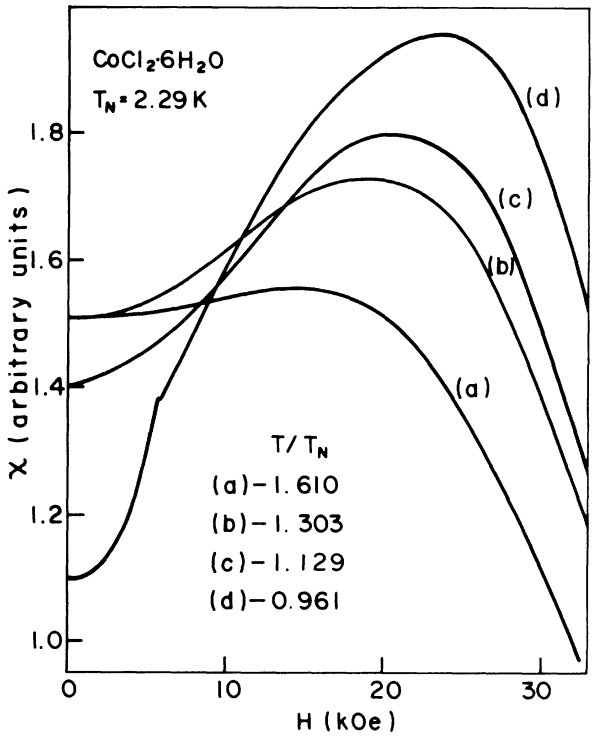

FIG. 1. Susceptibility of $CoCl_2\cdot 6H_2O$ as a function of the applied magnetic field at different temperatures.

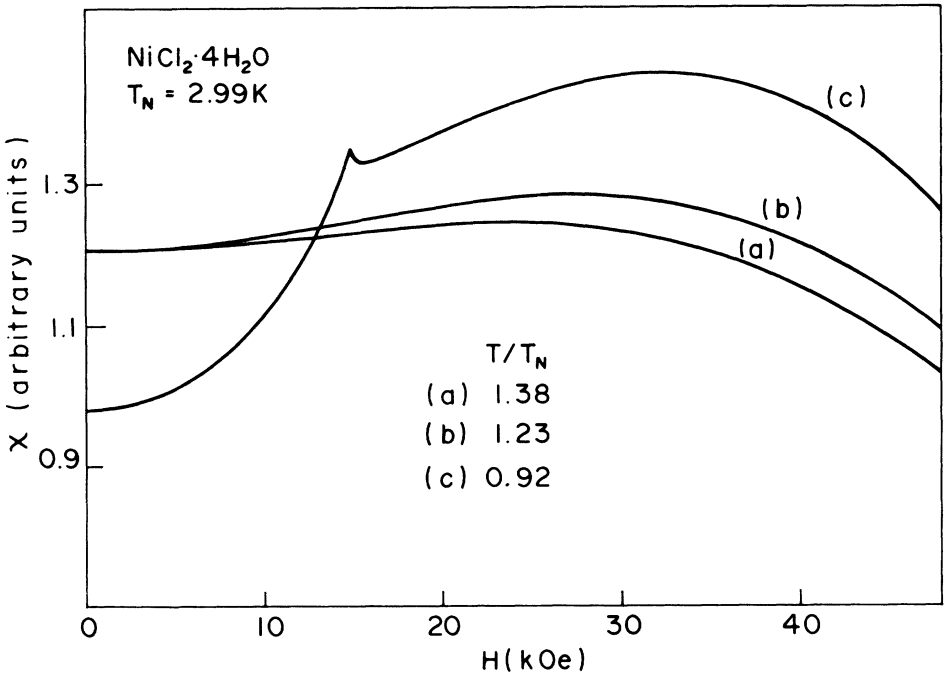

FIG. 2. Susceptibility of $NiCl_2 \cdot 4H_2O$ as a function of the applied magnetic field at different temperatures.

crease in height and occur at higher field values as the temperatures are lowered. Note that in the curves for $T < T_N$ (T_N is the critical temperature for $H=0$) this maximum persists. Also, these curves display, at lower field, a small knee. This anomaly corresponds to the continuous paramagnetic-antiferromagnetic transition. With a further decrease in temperature the location of the knee increases quickly in field and the knee evolves into a peak that outgrows the broad maximum of the

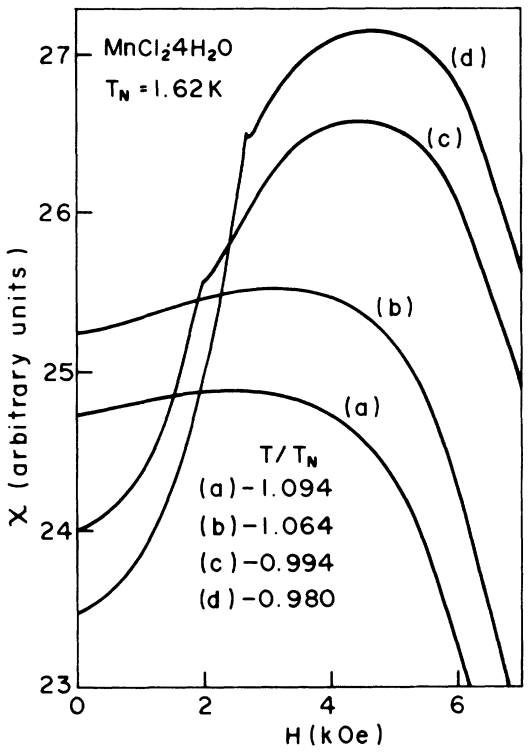

FIG. 3. Susceptibility of $MnCl_2 \cdot 4H_2O$ as a function of the applied magnetic field at different temperatures.

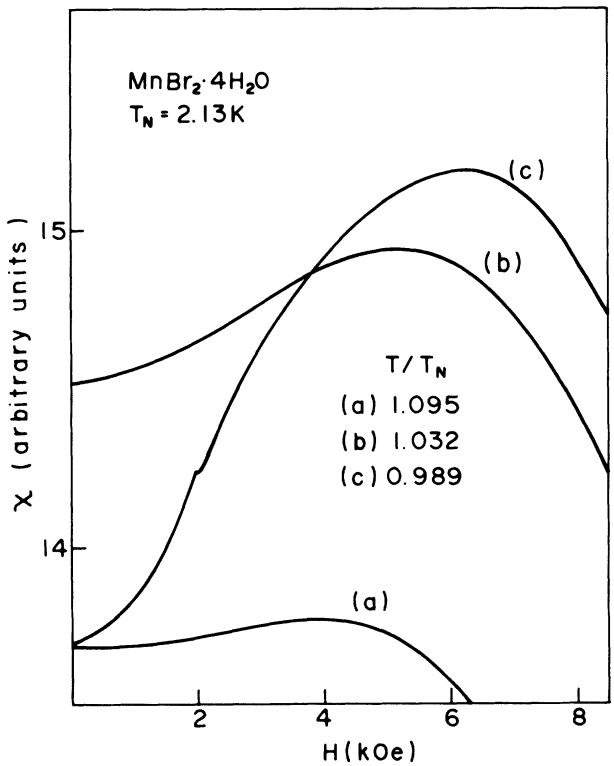

FIG. 4. Susceptibility of $MnBr_2 \cdot 4H_2O$ as a function of the applied magnetic field at different temperatures.

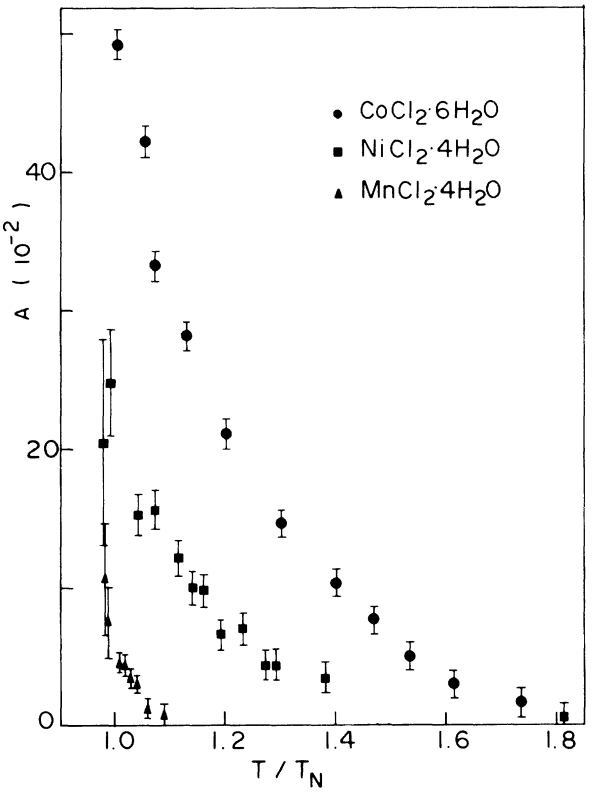

FIG. 5. Relative height of the susceptibility maximum $A=[\chi(m)-\chi(0)]/\chi(0)$ observed in the paramagnetic phase of the χ vs H curves plotted as a function of T/T_N. The data for $MnBr_2 \cdot 4H_2O$ is not displayed to avoid overcrowding.

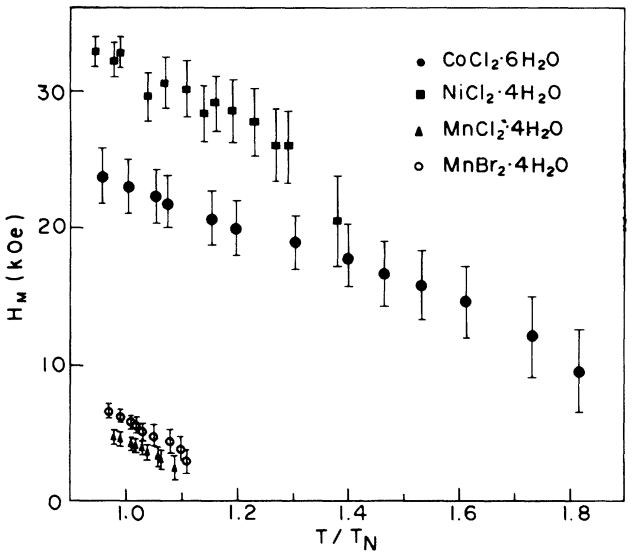

FIG. 6. Magnetic field H_M at which the maximum in the paramagnetic phase of the χ vs H curves occurs displayed as a function of the ratio T/T_N.

paramagnetic susceptibility.

In order to compare the intensity of this maximum for the different materials we consider the ratio $A=[\chi(m)-\chi(0)]/\chi(0)$ as a measure of this height. Here $\chi(m)$ is the maximum value of the paramagnetic susceptibility and $\chi(0)$ is its value at $H=0$. The results are displayed, as a function of T/T_N, in Fig. 5. To avoid overcrowding we did not report the results of $MnBr_2 \cdot 4H_2O$, which are of the same magnitude as those of $MnCl_2 \cdot 4H_2O$. For $T/T_N < 1$, a larger error is indicated in the figure. This is due to the fact that below T_N the ordering mechanism strongly reduces the value of the susceptibility at zero field, and $\chi(0)$ is approximately estimated from this data. The salient feature of this figure is that the effect is much greater in the cobalt compound ($S=\frac{1}{2}$) and persists at much higher temperatures.

Finally in Fig. 6 we plot the field values H_M, at which the maxima occur, as a function of T/T_N, for the four different compounds. The data for $CoCl_2 \cdot 6H_2O$ is in agreement with those obtained by Metselaar and De Klerk[5] who have reported two measurements in the temperature range of our interest. Note that H_M is higher for $NiCl_2 \cdot 4H_2O$ in the temperature interval $0.95 \leq T/T_N \leq 1.4$, but for $T/T_N > 1.4$ the effect is only observed in the Co compound.

V. DISCUSSION

Figures 5 and 6 summarize the main experimental results obtained. The striking feature of Fig. 5 is that the relative height of the paramagnetic susceptibility maximum is much higher in the cobalt

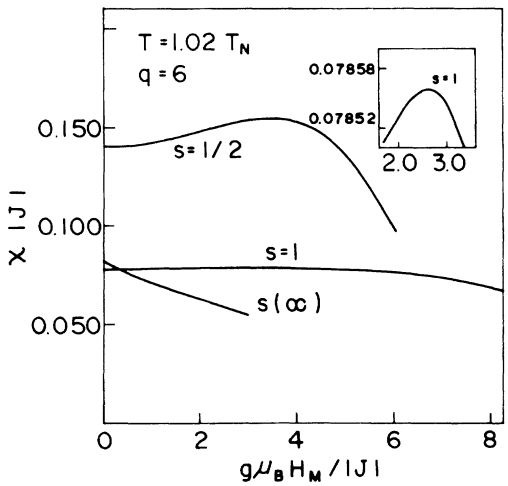

FIG. 7. Susceptibility as a function of $g\mu_B H_M/|J|$ calculated at $T/T_N=1.02$ using the variational method described in Appendixes A–C. These curves are for the isotropic Heisenberg model. The inset shows the details around the maximum for $S=1$.

($S=\frac{1}{2}$) compound and that this maximum persists at temperatures about twice T_N. This strongly suggests that the effect is enhanced in systems with lower spin values. In fact, our theoretical calculations (see Sec. II and Appendixes A–C) show that the paramagnetic susceptibility as a function of H exhibit a broad maximum for the isotropic Heisenberg ($q=6$) $S=\frac{1}{2}$ and $S=1$ systems. However, no evidence of this maximum was found for isotropic ($q=6$) systems with classical spins ($S=\infty$) in the low-field limit. These results are shown in Fig. 7 for a temperature $T/T_N=1.02$. It is clear that the relative height is much higher for $S=\frac{1}{2}$ than for $S=1$ (see inset in Fig. 7 for $S=1$). These calculations also indicate (see Figs. 8 and 9) that for $S=\frac{1}{2}$ the maximum of χ persists up to $T/T_N\sim 1.5$, whereas for $S=1$ it continues only up to $T/T_N\sim 1.1$.

The magnetic properties (susceptibility, phase diagrams, and specific heat) of $CoCl_2\cdot 6H_2O$ have been analyzed in terms of the two-dimensional (square-lattice) XY model.[5] Although the predictions based on the XY model cannot account for the observations very close to the critical point (specific-heat anomaly, etc.), correlated fluctuations responsible for the onset of long-range order (crossover to three-dimensional behavior) in the system are the dominant contributions. However, the analysis[5] shows good agreement between theory and experiment in the paramagnetic region (yielding a planar exchange constant $J/k=-4.10\pm 0.05k$), where short-range correlations within the XY layers are the dominant contributions and a two-dimensional behavior is expected. In order to simulate this two-dimensional character we have considered (see Appendix A) a planar XY model with $q=4$. Regardless of the fact that the XY model does not sustain long-range order in two dimensions,[19,20] we expect that the predicted paramagnetic susceptibility, in large part determined by the short-range correlations, provides a reasonable description of the field-dependent paramagnetic susceptibility of $CoCl_2\cdot 6H_2O$. In Fig. 8 we show A vs T/T_N calculated (see Appendix A) for the XY model with $S=\frac{1}{2}$ and $q=4$. It is clear that the effect is stronger in this case, reflecting the two-dimensional character of the short-range-order effects. On the other hand, Fig. 9 shows that $g\mu_B H_M/|J|$ is lower for low T, but the effect persists at much higher temperatures. This is experimentally observed, as evidenced in Fig. 6, by comparing the data for $CoCl_2\cdot 6H_2O$ ($S=\frac{1}{2}$) and $NiCl_2\cdot 4H_2O$ ($S=1$). To conclude the discussion of the $CoCl_2\cdot 6H_2O$ compound we compare (see Figs. 10 and 11) the theoretical predictions for A and H_M with the experimental data [using $J/k=-4.10$ K and $g=5.2$ (Ref. 5)]. With this value of J the calculated T_N [see Eq. (A7)] is 2.28 K in a probable fortuitous agreement with the experimental $T_N=2.29$ K. Very good agreement is also obtained for A vs T/T_N (see Fig. 11), whereas a qualitative one is obtained for H_M vs T/T_N (see Fig. 11). Note that A does not depend on the J and g values. These results are indicative that the two-dimensional XY model gives a reasonable description of the short-range correlations occurring in the paramagnetic phase of $CoCl_2\cdot 6H_2O$, as has previously been inferred from the temperature-dependent susceptibility data.[5]

In the previous discussions we considered isotropic Heisenberg and planar models. The effect of the anisotropy was not included. However, the experimental data for the $NiCl_2\cdot 4H_2O$ suggest that the

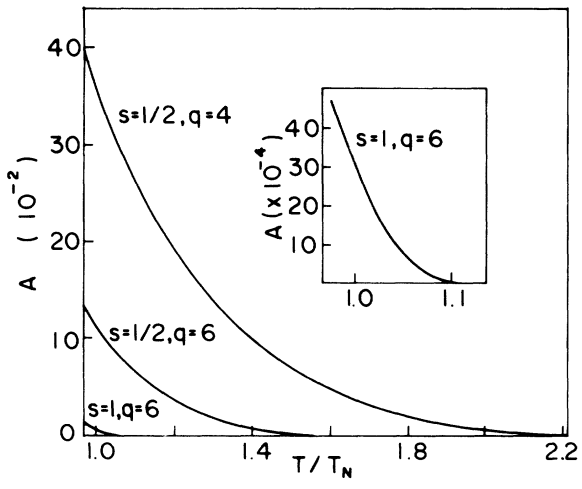

FIG. 8. Relative height of the susceptibility maximum $A=[\chi(m)-\chi(0)]/\chi(0)$ as a function of T/T_N for the isotropic Heisenberg model ($q=6$) and for the $S=\frac{1}{2}$, XY model ($q=4$). The inset shows the details of the results for $S=1$ Heisenberg model.

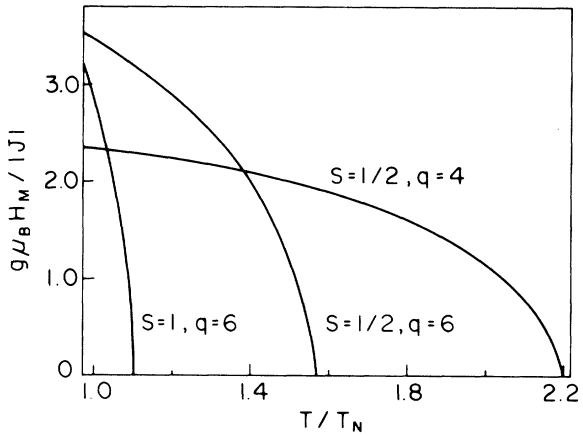

FIG. 9. Magnetic field H_M at which the maximum in the theoretical χ vs H curves occurs displayed as a function of T/T_N. The results are for the Heisenberg model ($q=6$) and for the $S=\frac{1}{2}$, XY model ($q=4$).

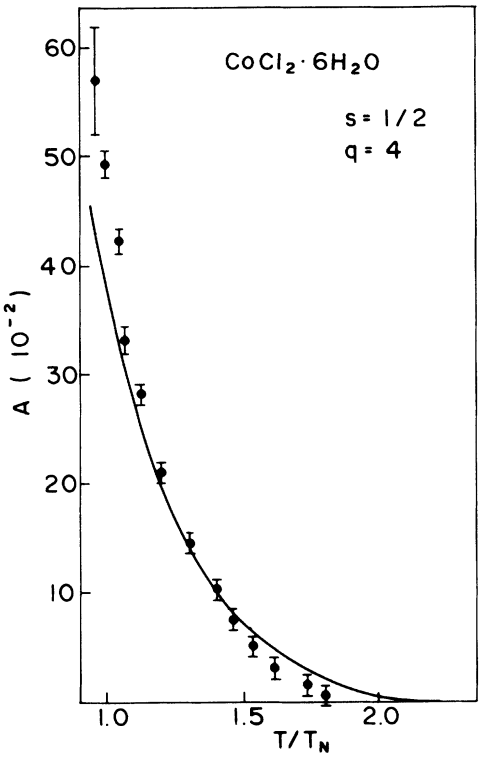

FIG. 10. Relative height of the susceptibility maximum $A=[\chi(m)-\chi(0)]/\chi(0)$ as a function of T/T_N for $CoCl_2 \cdot 6H_2O$. The solid lines are the theoretical predictions for $S=\frac{1}{2}$, XY model with $J/k=-4.10$ K and $g=5.2$.

mental data for the $NiCl_2 \cdot 4H_2O$ suggest that the short-range-order effects are much stronger than those calculated with the isotropic model and also that they extend up to higher values of T/T_N (see Fig. 5). We conjectured that these facts could result from the single-ion uniaxial anisotropy of this compound. Accordingly, we performed calculations with a $q=6$ and $S=1$ Heisenberg model in which a

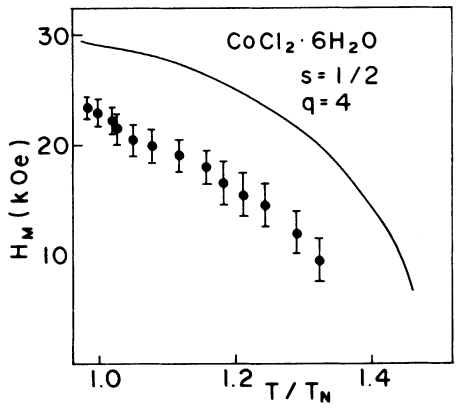

FIG. 11. Magnetic field H_M at which the maximum occurs as a function of T/T_N for $CoCl_2 \cdot 6H_2O$. The solid lines are the theoretical predictions for $S=\frac{1}{2}$, XY model with $J/k=-4.10$ K and $g=5.2$.

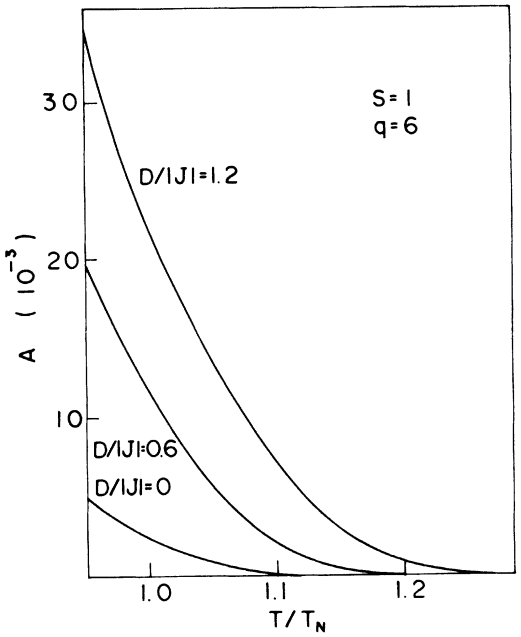

FIG. 12. Relative height of the susceptibility maximum as a function of T/T_N for the $S=1$ isotropic and anisotropic Heisenberg models ($q=6$).

single-ion term D was included. The predicted A and $g\mu_B H_M/|J|$ vs T/T_N curves for two values of the ratio $D/|J|$ are displayed in Figs. 12 and 13, respectively. For comparison, the isotropic case was also displayed. It is clear that the effect is stronger for higher D values. However, even for $D/|J|=1.2$,[16] the theoretical predictions for A and H_M, based on the anisotropic Heisenberg model, cannot quantitatively account for the observed experimental behavior. In particular, the predicted A, for $T/T_N=1$, is 1 order of magnitude less than the observed value. Also the observed effect persists up to much higher temperatures. We speculate that $NiCl_2 \cdot 4H_2O$ may have some two-dimensional character. One point in favor of this interpretation is that the maximum of χ, at zero field as a function of the temperature,[6] occurs at a temperature T_M, with $T_M/T_N \sim 1.25$. For tridimensional systems typical values for this ratio obtained from high-temperatures series expansions range from 1.05 to 1.1 T_M/T_N.[21]

Finally, we should note (see Fig. 6) that in the manganese compounds the effect is of the same order of magnitude and much less pronounced in comparison with the other two compounds. As there is a huge increase in the anisotropy (probable of exchange origin[22]) in going from the chloride to the bromide, we may conclude, from our data, that this fact has not strongly affected the effect. The small magnitude of it may be understood by the large spin

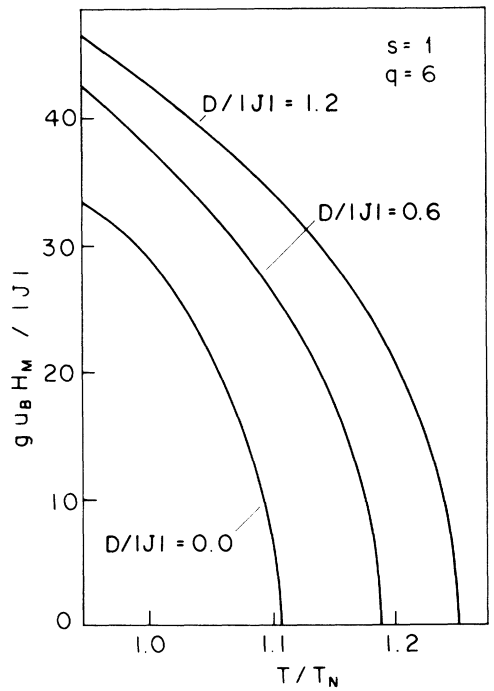

FIG. 13 Magnetic field H_M at which the maximum occurs as a function of T/T_N for the $S=1$ isotropic and anisotropic Heisenberg models ($q=6$).

value in both compounds, as theoretically expected (see Fig. 7).

In conclusion, we have shown that although the model calculations presented here were based on oversimplified Hamiltonians, the calculated magnetic susceptibilities explicitly revealed the dependence of the short-range-order effects on spin magnitude, lattice dimensionality, and anisotropy. The main indicative trends are in qualitative agreement with the experimental observations made in the four antiferromagnetic compounds.

ACKNOWLEDGMENTS

We gratefully acknowledge many helpful discussions with Professor M. J. Oliveira. We also acknowledge the financial support of the Brazilian agencies Fundação de Amparo à Pesquisa do Estado de São Paulo (FAPESP), Conselho Nacional de Desenvolvimento Cientifico e Tecnológico (CNPq), and Financiadora Nacional de Estudor e Projetos (FINEP).

APPENDIX A

Let us consider the spin-$\frac{1}{2}$ two-dimensional antiferromagnetic XY model as defined by Eq. (1). The trial Hamiltonian $\mathcal{H}_0=\mathcal{H}_{0f}+\mathcal{H}_{0p}$ [see Eq. (4)] is now given by

$$\mathcal{H}_{0f}=-\sum_A H_1^A S_x^A-\sum_B H_1^B S_x^B \tag{A1}$$

and

$$\mathcal{H}_{0p}=-\sum_{\text{pairs}}[J(S_x^A S_x^B+S_y^A S_y^B)+H_2^A S_x^A+H_2^B S_x^B]\,. \tag{A2}$$

The four parameters (molecular fields) are determined from the conditions over the sublattice magnetizations and from the minimization of ϕ with respect to the sublattice magnetizations. The relations obtained are

$$(1-q)H_1^A+qH_2^A=\gamma\,, \tag{A3}$$

$$\langle S_x^A\rangle=\frac{1}{\beta}\frac{\partial}{\partial H_1^A}\ln Z_1^A=\frac{1}{\beta}\frac{\partial}{\partial H_2^A}\ln Z_2\,, \tag{A4}$$

and similar relations for the sublattice B [$A\rightarrow B$ in Eqs. (A3) and (A4)]. Here $\beta=1/kT$, Z_1^A (Z_1^B) is the trial partition function of an isolated spin in sublattice A (B), and Z_2 is the trial partition function of a linked pair of spins, given by

$$Z_1^A=2\cosh\left[\frac{\beta H_1^A}{2}\right], \tag{A5}$$

$$\begin{aligned}Z_2=&\,2\exp\left[\frac{\beta}{|J|}H_2^A H_2^B\right]\\&+\exp\left[-\frac{\beta|J|}{2}\right]\exp\left[-\frac{\beta}{2|J|}(H_2^A+H_2^B)^2\right]\\&+2\exp\left[\frac{\beta|J|}{2}\right]\exp\left[\frac{\beta}{2|J|}(H_2^A-H_2^B)^2\right].\end{aligned} \tag{A6}$$

In zero field we have $H_1^A=-H_1^B=H_1$ and $H_2^A=-H_2^B=H_2$ (antiferromagnetic phase). From (A3) and (A4), with vanishing H_1 and H_2, we obtain an expression for the Néel temperature (T_N)

$$\frac{qK}{2}(2+e^{K/2}+e^{-K/2})=4(q-1)(e^{K/2}-1)\,, \tag{A7}$$

with $K=|J|/kT_N$. For $q=4$ (square lattice) we obtain $|J|/2kT_N=0.90$.

The susceptibility as a function of the applied field is calculated by differentiating the sublattice magnetization with respect to H. In the paramag-

netic region ($T \gtrsim T_N$), we take $\beta H_1^A = \beta H_1^B = 2x_1$ and $\beta H_2^A = \beta H_2^B = x_2$. We thus obtain the following expression:

$$\chi |J| = \frac{\beta |J| b_1 \mathrm{sech}^2 x_1}{2[2(1-q)b_1 + q\alpha^2 a_1^2 e^{\beta|J|}\mathrm{sech}^2 x_1]} , \tag{A8}$$

where

$$\alpha = \frac{1}{2}\left[\left[\frac{\beta|J|}{2}\right]^2 + (2x_2)^2\right]^{1/2} , \tag{A9}$$

$$a_1 = 1 + e^{\beta|J|/2} + 2e^{-\beta|J|/4}\cosh\alpha , \tag{A10}$$

$$b_1 = 2\left[\alpha a_1 + \frac{a_1}{2}(x_2)^2 - 2(x_2)^2 e^{-\beta|J|/4}\sinh\alpha\right] \times \sinh(2\alpha)(x_2)^2 a_1 \cos\alpha . \tag{A11}$$

x_1, x_2, and γ are related through [from Eqs. (A3) and (A4)]

$$\frac{\gamma}{|J|} = \frac{1}{\beta|J|}[2x_1(1-q) + qx_2] \tag{A12}$$

and

$$\tanh x_1 = \frac{2x_2 e^{-\beta|J|/4}\sinh\alpha}{2a_1} . \tag{A13}$$

APPENDIX B

For a spin-1 tridimensional isotropic Heisenberg antiferromagnet, the procedure is the same developed in Sec. II B. In this case the expression for the Néel temperature is

$$2qK(1+5e^{-3K}+3e^{-K}) = (q-1)(8-5e^{-3K}-3e^{-K}) , \tag{B1}$$

which is identical to that obtained using the constant-coupling approximation.[23] For $q=6$ we have $K=0.32$.

The field-dependent paramagnetic susceptibility is given by

$$\chi |J| = \frac{2\beta|J| b_2[\cosh(2x_1)+2]}{b_2(1-q)[1+2\cosh(2x_1)]^2 + 2qa_2^2[\cosh(2x_1)+2]} , \tag{B2}$$

where

$$a_2 = 2e^{-\beta|J|}\cosh(2x_2) + 4\cosh x_2 \cosh(\beta|J|) + e^{2\beta|J|} + 2\cosh(\beta|J|) \tag{B3}$$

and

$$b_2 = 2\{a_2[2e^{-\beta|J|}\cosh(2x_2) + \cosh x_2\cosh(\beta|J|)] - 4[e^{-\beta|J|}\sinh(2x_2) + \sinh x_2\cosh(\beta|J|)]^2\} . \tag{B4}$$

x_1, x_2, and γ are related through Eq. (A12) and [from (A4)]

$$\cosh(2x_1) = \frac{4y + (64-48y)^{1/2}}{8(1+y)} , \tag{B5}$$

where

$$y^{1/2} = \frac{2e^{-\beta|J|}\sinh(2x_2) + 2\sinh x_2\cosh(\beta|J|)}{a_2} . \tag{B6}$$

In the case of the spin-1 anisotropic Heisenberg antiferromagnet we consider the Hamiltonian (2). The trial Hamiltonian includes $N-2n$ free-spin terms

$$\mathcal{H}_{0f} = -\sum_A [H_1^A S_z^A + D(S_z^A)^2] - \sum_B [H_1^B S_z^B + D(S_z^B)^2] , \tag{B7}$$

and n pair terms

$$\mathcal{H}_{0p} = -\sum_{\text{pairs}} \{J\vec{S}^A\cdot\vec{S}^B + H_2^A S_z^A + H_2^B S_z^B + D[(S_z^A)^2 + (S_z^B)^2]\} . \tag{B8}$$

The sublattice magnetization is given by

$$\langle S_z^A\rangle = \frac{1}{\beta}\frac{\partial}{\partial H_1^A}\ln Z_1^A = \frac{1}{\beta}\frac{\partial}{\partial H_z^A}\ln Z_2 , \tag{B9}$$

where

$$Z_1^A = 1 + 2e^{\beta D}\cosh(\beta H_1^A)$$

and

$$Z_2=2e^{-\beta|J|+2\beta D}\cosh[\beta(H_2^A+H_2^B)]+4e^{\beta D}\cosh\left[\frac{\beta}{2}(H_2^A+H_2^B)\right]\cosh(\beta N)$$
$$+e^{-\beta(t_1+t_2)}\exp\left[\frac{4}{3}\left[\frac{\beta|J|}{2}+\beta D\right]\right]+2\exp\left[\frac{\beta}{2}(t_1+t_2)\right]\exp\left[\frac{4}{3}\left[\frac{\beta|J|}{2}+\beta D\right]\right]$$
$$\times\cosh\left[\frac{\beta i\sqrt{3}}{2}(t_1+t_2)\right], \tag{B10}$$

where

$$N=\tfrac{1}{2}[(H_2^A-H_2^B)^2+4|J|^2]^{1/2}, \tag{B11}$$
$$t_1=(r+M)^{1/2}, \tag{B12}$$
$$t_2=(r-M)^{1/2}, \tag{B13}$$
$$r=\tfrac{1}{27}[10|J|^3+24|J|^2D+8D^3-9(|J|+2D)(H_2^B-H_2^A)^2], \tag{B14}$$
$$M^2=\tfrac{1}{27}[-9|J|^6-4|J|^5D-4|J|^4D-(H_2^B-H_2^A)^2(23|J|^4+48|J|^3D+64|J|^2D^2+32|J|D^3+16D^4)$$
$$+(H_2^B-H_2^A)^4(-4|J|^2+8|J|D+8D^2)-(H_2^B-H_2^A)^6]. \tag{B15}$$

We choose again $n=Nq/2$ by comparison with the first terms of the high-temperature expansion. For simplicity, we take $K=0.32$, as in the isotropic case. From the minimization of ϕ with respect to the sublattice magnetizations and Eq. (B9), we obtain the following equation for the field-dependent paramagnetic susceptibility

$$\chi|J|=\frac{2\beta|J|e^{D/|J|}[\cosh(2x_1)+2e^{D/|J|}]a_3}{qb_3^2e^{D/|J|}[\cosh(2x_1)+2e^{D/|J|}]+(1-q)a_3[1+2e^{D/|J|}\cosh(2x_1)]} \tag{B16}$$

where

$$a_3=b_3[2e^{-\beta|J|+2D/|J|}\cosh(2x_2)+e^{D/|J|}\cosh(\beta|J|)\cosh x_2]-4c^2, \tag{B17}$$
$$b_3=2e^{-\beta|J|+2D/|J|}\cosh(2x_2)+4e^{D/|J|}\cosh(x_2)\cosh(\beta|J|)+e^{\beta|J|+2D/|J|}$$
$$+2e^{\beta|J|/2+\beta/|J|}\cosh\left[\left[\frac{\beta|J|}{2}+\frac{D}{|J|}\right]^2+2(\beta|J|)^2\right], \tag{B18}$$
$$c=e^{-\beta|J|+2D/|J|}\sinh(2x_2)+e^{D/|J|}\cosh(\beta|J|)\sinh(x_2), \tag{B19}$$

as in the previous cases, x_1, x_2, and γ are related through Eq. (A12) and [from (A4)]

$$\cosh(2x_1)=\frac{d+[4e^{2D/|J|}(1-d)+d]^{1/2}}{2e^{D/|J|}(1-d)}, \tag{B20}$$

where

$$d=\frac{4c^2}{b_3^2}. \tag{B21}$$

APPENDIX C

Finally we developed the variational procedure to study the behavior of the field-dependent paramagnetic susceptibility of an antiferromagnet with infinite spin, according to the Hamiltonian (3). In a similar way, as developed in the previous cases, we consider a trial Hamiltonian, $\mathcal{H}_0=\mathcal{H}_{0f}+\mathcal{H}_{0p}$, where

$$\mathcal{H}_{0f}=-\sum_A H_1^A s_z^A-\sum_B H_1^B s_z^B \tag{C1}$$

and

$$\mathcal{H}_{0p}=-\sum_{\text{pairs}}(J\vec{s}^A\cdot\vec{s}^B+H_z^A s_z^A+H_2^B s_z^B). \tag{C2}$$

In this case the partition functions are

$$z_1^A=\int_0^{2\pi}d\psi\int_0^{\pi}d\theta\sin\theta e^{\beta H_1^A\cos\theta}=\frac{4\pi}{\beta H_1^A}\sinh(\beta H_1^A) \tag{C3}$$

and

$$Z_2=\int_0^{2\pi}d\psi_A\int_0^{\pi}d\theta_A\sin\theta_A\int_0^{2\pi}d\psi_B\int_0^{\pi}d\theta_B\sin\theta_B(e^{\beta J\vec{s}^A\cdot\vec{s}^B}e^{\beta H_2^A s_z^A}e^{\beta H_2^B s_z^B}), \tag{C4}$$

where the direction of each spin is denoted by (θ_i,ψ_i). We calculate ϕ and choose $n=Nq/2$ by comparison between the first terms of the high-temperature expansion of ϕ and the exact high-temperature expansion. From the minimization of ϕ with respect to the sublattice magnetizations we obtain

$$(1-q)H_1^A+qH_2^A=\gamma\,, \tag{C5}$$

and a similar relation for the sublattice B.

To calculate the Néel temperature and the susceptibility as a function of the field we expand Z_2 in a series of modified spherical Bessel functions of the second kind and take the small-field limit. For T_N we obtain the following equation:

$$L(K)=\frac{1}{q-1}\,, \tag{C6}$$

where $L(K)$ is the Langevin function. This is the Néel temperature of a "Bethe lattice" of coordination number q.[9]

The field-dependent paramagnetic susceptibility for small fields is given by

$$\chi=\frac{\beta[\frac{1}{3}+\frac{1}{3}L(a_4)+\frac{1}{5}\beta H_2L(a_4)]}{1+(1-q)L(a_4)+\frac{3}{5}(1-q)\beta H_2L(a_4)}\,, \tag{C7}$$

where

$$a_4=-\beta|J| \tag{C8}$$

and

$$H_2=\frac{1}{1+(1+q)L(a_4)}\,. \tag{C9}$$

[1]C. C. Becerra, Ph.D. thesis, University of São Paulo, 1974 (unpublished).

[2]A. Paduan Filho and N. F. Oliveira, Jr., Chem. Solids 37, 251 (1976).

[3]D. P. Landau, B. E. Keem, B. Schneider, and W. P. Wolf, Phys. Rev. B 3, 2310 (1971).

[4]L. G. Ferreira, S. R. Salinas, and M. J. Oliveira, Phys. Status Solidi B 83, 229 (1977).

[5]J. W. Metselaar and D. De Klerk, Physica (Utrecht) 63, 191 (1973); J. W. Metselaar, L. J. De Jongh, and D. De Klerk, Physica 79B, 53 (1975); L. J. De Jongh and A. R. Miedema, Adv. Phys. 23, 1 (1974).

[6]J. N. McElearney, D. B. Losee, S. Mechant, and R. L. Carlin, Phys. Rev. B 7, 3314 (1973).

[7]H. M. Gijsmann, N. J. Poulis, and J. Van den Handel, Physica (Utrecht) 25, 954 (1959).

[8]C. C. Becerra, A. Paduan Filho, and N. F. Oliveira, Jr., Solid State Commun. 16, 791 (1975).

[9]M. E. Fisher, Am. J. Phys. 32, 343 (1964).

[10]J. S. Smart, *Effective Field Theories of Magnetism* (Saunders, Philadelphia, 1966).

[11]P. Groth, *Chemische Krystallograpie* (Engelman, Leipzig, 1908), Vol. 1.

[12]W. K. Robinson and S. A. Friedberg, J. Appl. Phys. 31, 3385 (1960).

[13]T. Haseda, J. Phys. Soc. Jpn. 15, 483 (1960); R. B. Flippen and S. A. Friedberg, J. Appl. Phys. 31, 338s (1960).

[14]S. Spooner, R. F. Altman, and K. Sudarsanan, *American Crystallographic Association Summer Meeting—1971, Ames, Iowa* (American Crystallographic Association, New York, 1971), p.99.

[15]R. F. Altman, S. Spooner, D. P. Landau, and J. E. Rives, Phys. Rev. B 11, 458 (1975); R. A. Butera and D. R. Rutter, J. Appl. Phys. 49, 1344 (1978).

[16]A. Paduan Filho, C. C. Becerra, and N. F. Oliveira, Jr., Phys. Lett. 50A, 51 (1974).

[17]E. Maxwell, Rev. Sci. Instrum. 36, 553 (1965).

[18]N. F. Oliveira, Jr. and C. J. Quadros, J. Phys. E 2, 967 (1969).

[19]N. D. Mermin and H. Wagner, Phys. Rev. Lett. 17, 1133 (1966).

[20]For a discussion of two-dimensional behavior in magnetic systems, see, e.g., J. M. Kosterliz and D. J. Thouless, in *Progress in Low Temperature Physics*, edited by D. F. Brewer (North-Holland, Amsterdam, 1978), p.371.

[21]M. E. Fisher and M. F. Sykes, Physica (Utrecht) 28, 939 (1962).

[22]C. H. Westphal and C. C. Becerra, J. Phys. C 15, 6221 (1982).

[23]J. van Kranendonk and P. W. Kasteleijn, Physica (Utrecht) 22, 317 (1956).